Received: 10 August 2016 | Revised: 5 January 2017 | Accepted: 15 January 2017

DOI 10.1002/tox.22402

RESEARCH ARTICLE

WILEY ENVIRONMENTAL TOXICOLOGY

Preventive effects of *Ophiocordyceps sinensis* mycelium on the liver fibrosis induced by thioacetamide

Yi-Hsieng Samuel Wu[1]* | Jung-Kai Tseng[2,3]* | Chung-Hsi Chou[4,5] | Chih-Hsien Chiu[1] | Yi-Ling Lin[1] | Yi-Chen Chen[1,5]

[1]Department of Animal Science and Technology, National Taiwan University, Taipei 106, Taiwan

[2]Department of Optometry, Asia University, Taichung 413, Taiwan

[3]Department of Medical Research, China Medical University Hospital, China Medical University, Taichung 404, Taiwan

[4]School of Veterinary Medicine, National Taiwan University, Taipei 106, Taiwan

[5]Zoonoses Research Center, National Taiwan University, Taipei 106, Taiwan

Correspondence
Yi-Chen Chen, Department of Animal Science and Technology, National Taiwan University, Taipei 106, Taiwan.
Email: ycpchen@ntu.edu.tw

Abstract

Thioacetamide (TAA), usually used as a fungicide to control the decay of citrus products, itself is not toxic to the liver, but its intermediates are able to increase oxidative stress in livers and further cause fibrosis. *Ophiocordyceps sinensis* mycelium (OSM) which contains 10% polysaccharides and 0.25% adenosine decreased ($P < 0.05$) the lipid accumulation and increased ($P < 0.05$) antioxidative capacity in livers of thioacetamide (TAA) injected rats. Meanwhile, the increased ($P < 0.05$) liver sizes, serum alanine transaminase (AST) and aspartate transaminase (ALT) values in thioacetamide (TAA)-injected rats were ameliorated ($P < 0.05$) by OSM supplementation. Moreover, the levels of proinflammatory cytokines, such as the tumor necrosis factor-α (TNF-α) and interleukin-1β (IL-1β), were also reduced ($P < 0.05$). The fibrosis phenomena in pathological (Masson's trichrome and H&E stainings) and immunohistochemical [α-smooth actin (αSMA) and CD86/ED1] observations in TAA-treated rats were reduced ($P < 0.05$) by OSM cotreatment. The protective effect of OSM against TAA-induced liver inflammation/fibrosis may be via downregulations ($P < 0.05$) of TGF-β pathways and NFκB which further influenced ($P < 0.05$) the expressions of fibrotic and inflammatory genes (i. e., αSMA, Col1α, COX2). Therefore, OSM shows preventive effects on the development of TAA-induced hepatic fibrosis.

KEYWORDS

antioxidative capacity, liver inflammation/fibrosis, *Ophiocordyceps sinensis* mycelium, thioacetamide

1 | INTRODUCTION

Liver fibrosis is a chronic liver damage usually caused by alcohol, viruses or other toxins. It is characterized by an excessive accumulation of extracellular matrix (ECM) proteins such as collagen, and the ECM is mainly secreted by myofibroblast-like hepatic stellate cells (also called activated HSCs). Haloalkanes such as chloroform, iodoform, and carbon tetrachloride have been recognized as environmental chemical inducers of hepatic fibrosis.[1] Thioacetamide (CH_3-C(S)NH_2, TAA), usually used as a fungicide to control the decay of citrus products, and has been characterized as a hepatotoxin.[2] Actually, TAA itself is not toxic to the liver, but its intermediates (i. e., thioacetamide-*S*-oxide or thioacetamide-*S*, *S*-dioxide via the cytochrome P450 (CYP2E1) and/or flavin-containing monooxygenase (FMO) systems) are able to covalently bind to hepatic macromolecules and eventually initiate necrosis of liver cells.[3]

In 1993, the year of summer Olympic game, *Ophiocordyceps sinensis* (OS, renamed from *Cordyceps sinensis* in 2007) first gained a worldwide attention when it was revealed that several Chinese laureates included it in their diet.[4]. Researchers have indicated that OS showed remarkable hepatoprotective effects, especially anti-inflammation[5] and anti-fibrosis.[6] However, its rareness and expensiveness restrict the prevalence of application. Hence, most of following studies focused on identification, cultivation, and bioactive effects of that edible *Ophiocordyceps sinensis* mycelium (OSM), which comes from an artificial cultivation system. Anticipatedly,[7] reported that polysaccharides from OSM can activate the mouse RAW264.7 macrophage cell and modulate its cytokine secretion under lipopolysaccharide induction. Peng et al.[8] indicated that OSM protects liver sinusoidal endothelial cells in lipopolysaccharide/D-galactosamine induced mice, and its protective mechanism was involved modulation of matrix metalloproteinases (MMP)−2/9 activities and anti-oxidative capability. Besides, a previous research showed that the OSM water extracts could ameliorate liver acute damage against carbon

*Yi-Hsieng Samuel Wu and Jung-Kai Tseng contributed equally to this work.

tetrachloride (CCl_4)-induction in rats. Furthermore, the anti-fibrotic effect of OSM has been proved to be associated with its down-regulation on the HSC activation.[9] However, the interactions of these multiple signal transductions during the fibrotic development are still lacking.

Although many OSM-origin bioactive compounds, that is peptide, ergosterol, polysaccharides, and so forth, perform hepatoprotective, the certain molecular mechanism of each or combination against the development of fibrotic livers is still undetermined. Because of the diverse structures of polysaccharides, the major ingredient (3–8%) among others of OSM, were regarded as the most possible bioactive compound which contributing the anti-inflammation.[10] Hence, this investigation examined the protective effect of OSM (containing 10% polysaccharides and 0.25% adenosine) via collecting physiological parameters, blood biochemical, and pathohistological analyses, and meanwhile, approached the possible modulation between the transforming growth factor beta 1 (TGF-β1) and nuclear factor kappa-light-chain-enhancer of activated B cells (NFκB) pathway in livers of TAA-injected rats under OSM consumption.

2 | MATERIALS AND METHODS

2.1 | Chemicals and *Ophiocordyceps sinensis* mycelium (OSM)

TAA were purchased from Sigma–Aldrich (St. Louis, MO). As a fibrogenic hepatoxin, TAA was dissolved in sterile phosphate-buffered saline (PBS). *Ophiocordyceps sinensis* mycelium (OSM) powder is a major component (72.82%) in TCM-808FB® powder (TCM Biotech International, Taipei, Taiwan) and others are excipients, that is, phosphate powder, magnesium steatate, silicon dioxide, and pregelatinized potato starch. TCM-808FB® powder contains approximate 10% polysaccharides and 0.25% adenosine. All mentioned chemicals without any indication in the context were purchased from Sigma–Aldrich. (St. Louis, MO).

2.2 | Animal and treatments

A total 48 male Wistar rats (6-weeks old) between 250 and 300 g were purchased from BioLASCO Taiwan (Taipei, Taiwan). Two rats were housed in one cage under the condition of 22°C ± 2°C, ~60 to 80% relative humidity, and 12 h light-dark cycle. All rats were acclimatized for 1 week prior to the experimental treatment. Rats were randomly divided into four groups: (1) Control: saline (i.p.) and distilled water (gavage); (2) TAA: TAA (100 mg kg^{-1} BW, i.p.) and distilled water (gavage); (3) OSML: TAA (100 mg kg^{-1} BW, i.p.) and OSM (280.8 mg TCM-808FB kg^{-1} BW, gavage); (4) OSMH: TAA (100 mg kg^{-1} BW, i.p.) and OSM (1404 mg TCM-808FB kg^{-1} BW, gavage). OSM powder dosages used in this study was according to the polysaccharide contents in OSM from Peng et al.[9] TAA and OSM treatments were both given three times per week during a persistent 8-week period. Water and diet were given *ad libitum*. Animal use and protocol were approved by the National Taiwan University Institution Animal Care and Use Committee (IACUU No.: 100-015).

2.3 | Sample collection and preparation of liver homogenate

During the experimental period, food and water intakes as well as body weights were recorded weekly. At the end of experiment, the blood samples of euthanized rats were harvested by an abdominal aorta puncture. The heart, liver, and kidney from each rat were removed and weighted individually. Livers were cut and soaked in 10% formalin for histopathological analyses, and the remnants were placed into liquid N_2. A 0.5 g of liver was homogenized on ice in 4.5 mL of PBS (pH 7.0, containing 0.25 M sucrose) and centrifuged at 12,000*g* for 30 min (Model 3740; KUBOTA, Tokyo, Japan). The supernatant was collected for further analyses. The protein content in the supernatant was measured according to the procedures of a Bio-Rad protein assay kit (catalog #500-0006; Bio-Rad Laboratories, Hercules, CA) using bovine serine albumin as a standard.

2.4 | Serum biochemical value and liver lipid analyses

Blood samples were placed for clotting, and supernatant were collected after a centrifugation at 3,000*g* for 15 min (Model 3740; KUBOTA, Tokyo, Japan). The serum alanine aminotransferase (ALT; GPT), aspartate aminotransferase (AST; GOT), albumin (ALB), triglyceride, and cholesterol levels were measured by using an ARKRAY SPOTCHEM SP-4410 automatic dry chemistry analyzer (ARKRAY, Tokyo, Japan) with respective kits.

Liver triglyceride and cholesterol concentrations were measured according to procedures of a previous report.[11] Briefly, liver lipid was extracted by chloroform and methanol (2:1, v/v). The extract was dried under N_2 and resuspended in isopropanol via an ultrasonic cleaner (Model: DC150H, Taiwan Delta New Instrument, Taiwan). Liver triglyceride and cholesterol levels were measured via commercial kits (Randox Laboratories, Antrim, United Kingdom).

2.5 | Liver antioxidative capability and cytokine analyses

The liver thiobarbituric acid reactive substances (TBARS) was used to represent the level of liver lipid peroxidation while glutathione (GSH), trolox equivalent antioxidant capacity (TEAC), and activities of superoxide dismutase (SOD), catalase (CAT), and glutathione peroxidase (GPx) were assayed as indices for liver antioxidative capacities. They all were performed according to procedures described by Fang et al.[11]

Liver TNF-α (Quantikine Rat TNF-α immunoassay, CAT: RTA00) and IL-1β (Quantikine Rat IL-1β/IL-1F2 immunoassay, CAT: RLB00) contents were measured by sandwich enzyme-linked immunosorbent assay (ELISA) and the procedures were followed according to the manual instructions (R&D system, Minneapolis, MN). The optical density value of each well was measured in an ELISA reader (BioTek Instruments, Winooski, VT). Hepatic TNF-α and IL-1β levels were both expressed by pg mg^{-1} protein.

2.6 | Histopathological sections and staining

Liver tissues were soaked in formalin, and the solution was renewed after 24 h. Dehydration series in graded alcohol and xylene were conducted,

consequently, tissues were embedded in paraffin wax (Leica Microsystems, Singapore) as block, which were sliced via a HM315R microtome (Thermo Fisher Scientific, Waltham, MA). All slides underwent opposite procedure of dehydration series, and stained with hematoxylin (Merck Millipore, Darmstadt, Germany) and eosin (Merck Millipore), or Masson's trichrome (Product No. HT15, Sigma–Aldrich, St. Louis, MO).

The liver fibrotic and inflammatory scores were given by trained observers. The METAVIR fibrosis staging system that contains five levels (one to five points) depending on the fibrotic severity of sample.[12] The histology activity index score (HAI score) was also applicate to determine the activities of inflammatory levels according to area condition such as portal inflammation (0, 1, 3, and 4 points), intralobular degeneration (0, 1, 3, and 4 points), and periportal-bridging necrosis (0, 1, 3, 4, 5, 6, and 10 points).[12]

2.7 | Immunohistochemical analyses

Immunohistochemical assay were conducted via VECTOR kit (VECTOR Laboratories, Peterborough, United Kingdom) (Mouse IgG, PK-6102; Rabbit IgG, PK-6101). The procedures were according to the manual instructions. Before the immunochemical reaction, all tissue slices should be deparaffinized and hydrated as those in Histopathological Sections and Staining section. Antigen retrieval was processed in aqueous solution (10 mM sodium-citrate with 0.05% Tween-20) by autoclaving (120–122°C) for 2 min. Next, intrinsic signals were blocked via a biotin/avidin blocking kit (SP-2001; VECTOR Laboratories, Burlingame, CA) and H_2O_2/methanol buffer. Blocking with the buffer which contains the serum of host animal was conducted overnight. In addition, the slides underwent each 5-min wash in PBS four times between each aforesaid step.

Slides were incubated with primary antibody (CD68/ED1, sc-59103, SANTACRUZ BIOTECHNOLOGY, Dallas, TX; anti-Actin, smooth muscle, clone ASM-1, CBL171, Merck Millipore) diluted to an optimal concentration, and added the biotinylated secondary antibody solution for optimal time. Next, all slides were incubated with VECTASTAIN® Elite ABC reagent. Last, they were hybridized with DAB peroxidase substrate (Cat. No. SK-4100, VECTOR Laboratories), and counterstained, cleaned as well as mounted up. The microphotography was taken via a SAGE VISION IHD 4600 system with ToupView software (SAGE VISION, Taipei, Taiwan).

2.8 | Realtime PCR

About 0.1 g liver tissue was kept in 0.5 mL RNA later (Qiagen, Valencia, CA). The E.Z.N.A™ Tissue RNA kit (Omega Bio-Tek, Norcross, GA), and the cDNA was synthesized according to the manufacturer's protocol offered by ImProm-II™ Reverse Transcriptase (Promega, Madison, WI). All the primers as following were designed for the specific gene sequences: glyceraldehyde 3-phosphate dehydrogenase (*Gapdh*, GenBank No.: NM_017008.4) sense, 5′-GACCCCTTCATTGACCTCAAC-3′, antisense, 5′-GGAGATGATGACCCTTTTGGC-3′; transforming growth factor beta 1 (*Tgfb1*, GenBank No.: NM_021578.2) sense, 5′- CTTTGTA CAACAGCACCCGC-3′, antisense, 5′- TAGATTGCGTTGTTGCGGTC-3′; transforming growth factor beta receptor 1 (*Tgfbr1*, GenBank No.: NM_012775.2) sense, 5′- TCCAAACCACAGAGTAGGCAC-3′, antisense, 5′-TGGATTCCGCCAATGGAACA-3′; transforming growth factor beta receptor 2 (*Tgfbr2*, GenBank No.: NM_031132.3) sense, 5′- CCGTGTG GAGGAAGAACGAC-3′, antisense, 5′-TGAAGCCGTGGTAGGTGAAC-3′; toll-like receptor 4 (*Tlr4*, GenBank No.: NM_019178.1) sense, 5′-CTACCTCGAGTGGGAGGACA-3′, antisense, 5′-TGGGTTTTAGGCGCA GAGTT-3′; TIR-domain-containing adapter-inducing interferon-β (*Trif*, GenBank No.: NM_053588.2) sense, 5′-CCTATGTCGCGGAAGTGTGA-3′, antisense, 5′- TGCAGCTACCAGAAACCCTC-3′; Myeloid differentiation primary response 88 (*Myd88*, GenBank No.: NM_198130.1) sense, 5′-CTCGCAGTTTGTTGGATGCC-3′, antisense, 5′-TCGATGCGGTCCTT CAGTTC-3′; Smooth muscle α-actin (*αSMA*, GenBank No.: NM_031004.2) sense, 5′- AGAAGCTGCTCCAGCTATGTG-3′, antisense, 5′- ATCACTCCCTGGTGTCTGGG-3′; Collagen, type I, alpha 1 (*Col1a1*, GenBank No.: NM_053304.1) sense, 5′- GACTGTCCCAACCCCCAAAA-3′, antisense, 5′- CTTGGGTCCCTCGACTCCTA-3′; nuclear factor kappa-light-chain-enhancer of activated B cells (*Nfkb*, GenBank No.: NM_001276711.1) sense, 5′-TGGGGCCTGCAAAGGTTATC-3′, antisense, 5′-TTTGCAAAGCCAACCACCAT-3′; cyclooxygenas 2 (*Cox2*, GenBank No.: NM_017232.3) sense, 5′- TGTATGCTACCATCTGGCT-3′, antisense, 5′- GTTTGGAACAGTCGCTCGTCATC-3′. Two μL cDNA (50 ng μL^{-1}), 5 μL Fast SYBR® Green Master Mix (Applied Biosystems, Framingham, MA), 2 μL RNase free water, and 1 μL primer were mixed together. The remnant was spun down by 1350*g* for 3 min (KUBOTA8700, KUBOTA, Tokyo, Japan; Rotor RS-3000/6 053-5930). The fluorescence signals of each target gene were detected by using the StepOne Real time PCR system (Applied Biosystems, Framingham, MA). *Gapdh* was used as an internal control, and the values of all genes in TAA, OSML, and OSMH rats were expressed relatively to the average value of Control rats, which was set to 1.0.

2.9 | Statistical analysis

The experiment was conducted by using a completely randomized design (CRD). Data were analyzed using analysis of variance (ANOVA). The significant differences were determined at 0.05 probability level, and differences between treatments were tested using the Least Significant Difference (LSD) test. All statistical analyses of data were performed using SAS 9.0 (SAS Institute, 2002).

3 | RESULTS AND DISCUSSION

3.1 | Effects of OSM on physiological parameters of rats

No ($P > 0.05$) differences on initial body weights were observed among groups (Table 1). At the end of experiment, the average body weight of Control group was heavier ($P < 0.05$) than TAA-injected groups (TAA, OSML, and OSMH groups) (Table 1), but there were no ($P > 0.05$) differences on final body weights among TAA-injected groups. During the experimental period, the food intakes were also not ($P > 0.05$) different (Table 1), but water intakes of TAA-treated groups (43.24, 45.51, and

TABLE 1 Growth performance, relative organ sizes, and hepatic antioxidative capacities of the experimental rats

Group[b]	Control	TAA	OSML	OSMH
	Growth performance[a]			
Initial body weight (g)	227.29 ± 2.12a	233.28 ± 1.11a	228.10 ± 3.52a	231.91 ± 1.99a
Final body weight (g)	426.99 ± 10.99a	339.62 ± 10.63b	347.23 ± 4.69b	342.86 ± 7.60b
Food intake (g per rat per day)	26.77 ± 0.69a	24.31 ± 1.32a	24.81 ± 0.73a	26.46 ± 1.36a
Water intake (mL per rat per day)	54.29 ± 1.94a	43.24 ± 1.95b	45.51 ± 1.57b	43.89 ± 1.65b
	Relative size (mg/100 g body weight)[a]			
Heart	297.38 ± 6.83a	311.47 ± 9.80a	322.78 ± 8.30a	316.82 ± 9.66a
Liver	2459.16 ± 61.59c	3093.84 ± 76.10a	2855.06 ± 48.00b	2914.79 ± 107.01ab
Kidney	557.86 ± 17.06c	654.01 ± 19.27a	604.47 ± 12.95bc	627.93 ± 18.36ab
	Antioxidative capacity and enzymatic activities[a]			
TABRS (nmol MDA eq mg^{-1} protein)	0.45 ± 0.02c	2.38 ± 0.04a	1.62 ± 0.05b	1.63 ± 0.06b
Reduced GSH (nmol mg^{-1} protein)	60.67 ± 1.87a	60.55 ± 1.62a	60.91 ± 1.36a	63.44 ± 1.37a
TEAC (nmol mg^{-1} protein)	100.18 ± 3.11a	83.51 ± 3.04b	108.87 ± 3.66a	109.36 ± 4.98a
SOD (U mg^{-1} protein)	11.12 ± 0.41b	4.35 ± 0.09c	14.15 ± 0.19a	10.64 ± 0.26b
CAT (U mg^{-1} protein)	19.72 ± 0.39b	17.38 ± 0.36c	20.83 ± 0.43ab	20.97 ± 0.38a
GPx (nmol NADPH oxidized min^{-1} mg^{-1} protein)	36.16 ± 0.79a	23.54 ± 0.54d	28.21 ± 0.55c	30.71 ± 0.59b

[a]The data were given as mean ± SEM ($n = 12$, except food and water intakes, $n = 6$). Mean values without the same letters in each testing parameter indicate a significant difference ($P < 0.05$).
[b]Rats were randomly divided into four groups: (1) Control: saline (i.p.) and distilled water (gavage); (2) TAA: TAA (100 mg kg^{-1} BW, i.p.) and distilled water (gavage); (3) OSML: TAA (100 mg kg^{-1} BW, i.p.) and OSM (280.8 mg TCM-808FB kg^{-1} BW, gavage); (4) OSMH: TAA (100 mg kg^{-1} BW, i.p.) and OSM (1404 mg TCM-808FB kg^{-1} BW, gavage).

45.51 mL per rat per day for TAA, OSML, and OSMH groups, respectively) were less ($P < 0.05$) than those of Control group (54.29 mL per rat per day). Regarding relative organ sizes (Table 1), there were no ($P > 0.05$) differences on heart sizes, but liver and kidney sizes were increased ($P < 0.05$) in TAA-injected groups compared to those of Control group. An OSM administration generally decreased liver and kidney sizes in TAA-injected rats (OSML group: TAA group, $P < 0.05$), but those were still higher ($P < 0.05$) than those of Control group.

Liver fibrosis is a chronic liver damage usually caused by alcohol, viruses or other toxins. Actually, TAA, usually used as a fungicide to control the decay of citrus products, itself is not toxic to the liver, but its intermediates are able to covalently bind to hepatic macromolecules and eventually initiate necrosis of liver cells.[3] The growth performance is an important factor of liver injury; meanwhile, the body weight is the representative value for the metabolic efficiency. The results of body weight corresponded to those in the study of Ljubuncic et al.[13] In addition, serum ALB values were highly related to muscle mass changes.[14] According to our results, ALB levels were not ($P > 0.05$) altered among all groups (Table 2), which implies that decreased body weights by TAA intoxication in this study did not comprise muscle mass changes. In addition, the food intakes were consistent, so the decreased body weights of TAA-injected rats are due to a liver-related metabolic dysfunction possibly. TAA could cause renal damage during an induction of chronic liver damage in clinical and animal researches.[15] During the experimental period, the discrepancy of water intakes among the groups (Table 1) may be due to intrahepatic-nodules-caused portal hypertension under the pathological processing, accompanying with decreased efficiencies of filtration and sodium reabsorption.[16,17] Hence, it is reasonable that the increased kidney size and decreased water intake presented in this study (Table 1). Comprehensively, the hepatic hypertrophy and lighter body weight were observed on TAA-injected rats.[13] While these symptoms were caused by toxic metabolites of TAA (i. e., thioacetamide-*S*-oxide and thioacetamide-*S*,*S*-dioxide).[18] Our team also showed the lower body weight and larger liver size of TAA-injected mice, but cotreatment of silymarin reversed these observations.[19]. However, the reversal effects ($P < 0.05$) on kidney and liver sizes, and water intakes of TAA-injected rats by supplementing OSM were obviously demonstrated.

3.2 | Effects of OSM on serum lipid, liver lipids, and antioxidative capacities

At the end of the experiment, while lower ($P < 0.05$) serum TG and TC were measured in TAA group, OSM supplementation increased ($P < 0.05$) serum lipids, especially TC, where OSM supplementation (OSML and OSMH groups) normalized ($P < 0.05$) them to the level of Control group (Table 2). On the contrary, the liver TG and TC contents of TAA-injected groups were higher ($P < 0.05$) than those of Control

TABLE 2 Serum and liver lipid contents, as well as liver damage indices and cytokines of the experimental rats

Group[b]	Control	TAA	OSML	OSMH
	Serum lipids (mg dL^{-1})[a]			
Triglyceride	142.98 ± 5.45a	70.15 ± 3.72c	90.45 ± 4.07b	94.76 ± 4.25b
Cholesterol	103.99 ± 3.54a	86.01 ± 2.98b	106.50 ± 3.08a	108.96 ± 3.29a
	Liver lipids (mg g^{-1} liver)[a]			
Triglyceride	10.29 ± 0.07b	11.56 ± 0.29a	10.12 ± 0.15b	10.06 ± 0.28b
Cholesterol	2.44 ± 0.07c	4.51 ± 0.08a	2.76 ± 0.11b	2.70 ± 0.09b
	Liver damage index[a]			
AST (IU L^{-1})	120.50 ± 3.59c	287.42 ± 7.54a	130.17 ± 5.44bc	139.33 ± 3.47b
ALT (IU L^{-1})	36.67 ± 1.06c	114.92 ± 4.56a	35.08 ± 1.96c	55.83 ± 3.23b
ALB (g dL^{-1})	4.00 ± 0.10a	4.10 ± 0.10a	4.10 ± 0.10a	4.30 ± 0.10a
	Liver cytokines (pg mg^{-1} protein)[a]			
IL-1β	3.28 ± 0.12b	5.03 ± 0.12a	3.68 ± 0.20b	3.73 ± 0.19b
TNF-α	18.40 ± 0.98c	26.00 ± 0.85a	22.72 ± 0.84b	22.02 ± 0.71b

[a]The data were given as mean ± SEM ($n = 12$). Mean values without the same letters in each testing parameter indicate a significant difference ($P < 0.05$).

[b]Rats were randomly divided into four groups: (1) Control: saline (i.p.) and distilled water (gavage); (2) TAA: TAA (100 mg kg^{-1} BW, i.p.) and distilled water (gavage); (3) OSML: TAA (100 mg kg^{-1} BW, i.p.) and OSM (280.8 mg TCM-808FB kg^{-1} BW, gavage); (4) OSMH: TAA (100 mg kg^{-1} BW, i.p.) and OSM (1404 mg TCM-808FB kg^{-1} BW, gavage).

group, but OSM supplementation reduced ($P < 0.05$) them (Table 2). These results imply that OSM supplementation could normalize the disturbance of lipid metabolism in TAA-injected rats. In addition, the liver antioxidative capacities are shown on Table 1. Increased ($P < 0.05$) TBARS values were assayed in livers of TAA-injected groups (Table 1) compared to that of Control group, but decreased ($P < 0.05$) ones were observed when TAA-injected rats were supplemented with OSM (Table 1). Although there were no ($P > 0.05$) differences on liver reduced GSH contents among groups, rats injected by TAA without OSM (TAA group) had the lower ($P < 0.05$) liver TEAC value than Control rats. However, OSM supplementation normalized ($P < 0.05$) liver TEAC values in TAA-injected rats, and the values were even similar ($P > 0.05$) to that of Control group (Table 1). Similarly, the activities of liver antioxidative enzymes, including SOD, CAT, and GPx were decreased ($P < 0.05$) by TAA treatment, but they were reversed ($P < 0.05$) by OSM supplementation and even higher ($P < 0.05$) than those of Control group, especially SOD and CAT activities in OSML and OSMH group, respectively (Table 1).

Kaplowitz[20] indicated that the metabolites of TAA attribute to the liver injury due to covalent bond formation which causes nuclear stress, ER stress, mitochondria stress, and oxidative stress; therefore, the production and delivery efficiencies of apoprotein B and low-density lipoprotein are decreased, thus causing lower serum lipids but higher liver lipid accumulation.[21] In addition, oxidative stress was defined as the exposures of an excessive level of reactive oxygen species (ROS), which also lead to adverse effects on many cellular functions. Similarly, Chen et al. reported that the liver antioxidative capacities were decreased in TAA-intoxication (Table 1) while the hepatic lipid accumulation in TAA-injected rats was increased.[21] Correspondingly, the hepatoprotection of OSM against CCl_4 resulted in decreased serum AST and ALT values, concurrently, increased antioxidative capabilities via OSM supplementation were also observed.[22] Regarding to effects of OSM on exercised rats, *Ophiocordyceps sinensis* improved an exercise endurance capacity by activating not only the skeletal muscle metabolic regulators but also a coordinated antioxidative response.[23] Altogether, the results revealed that OSM supplementation could consolidate the antioxidative system against extrinsic factor induced oxidative stress.

3.3 | Effects of OSM on liver damage

As expected, TAA treatment resulted in increased ($P < 0.05$) liver damage indices (AST and ALT values) but did not ($P > 0.05$) influence ALB values compared to those of Control group while OSM supplementation decreased ($P < 0.05$) AST and ALT values (Table 2). Based on the results of liver cytokines, TAA treatment indeed raised ($P < 0.05$) hepatic TNF-α and IL-1β values (Table 2), but OSM supplementation decreased ($P < 0.05$) them. Regarding to histopathological analyses, the visible signs of fibrosis and intrahepatic inflammation were directly observed (Figure 1A). By microscopic images and a double-blind evaluation, the quantitative results showed that OSM supplementation alleviates ($P < 0.05$) the processing of liver damage (Figure 1). In the microscopic image of Masson's trichrome stainings, visible fibrotic scars and collagen deposition are strong evidences for fibrotic development in TAA group (Figure 1A), and those observations of TAA-injected groups were quantitatively reduced by the OSM supplementation (Figure 1B). For H&E staining, the values were determined based on the coverage of monocyte-aggregated region (black arrow), the amount of cells under necrosis (black triangle), the morphology of portal area

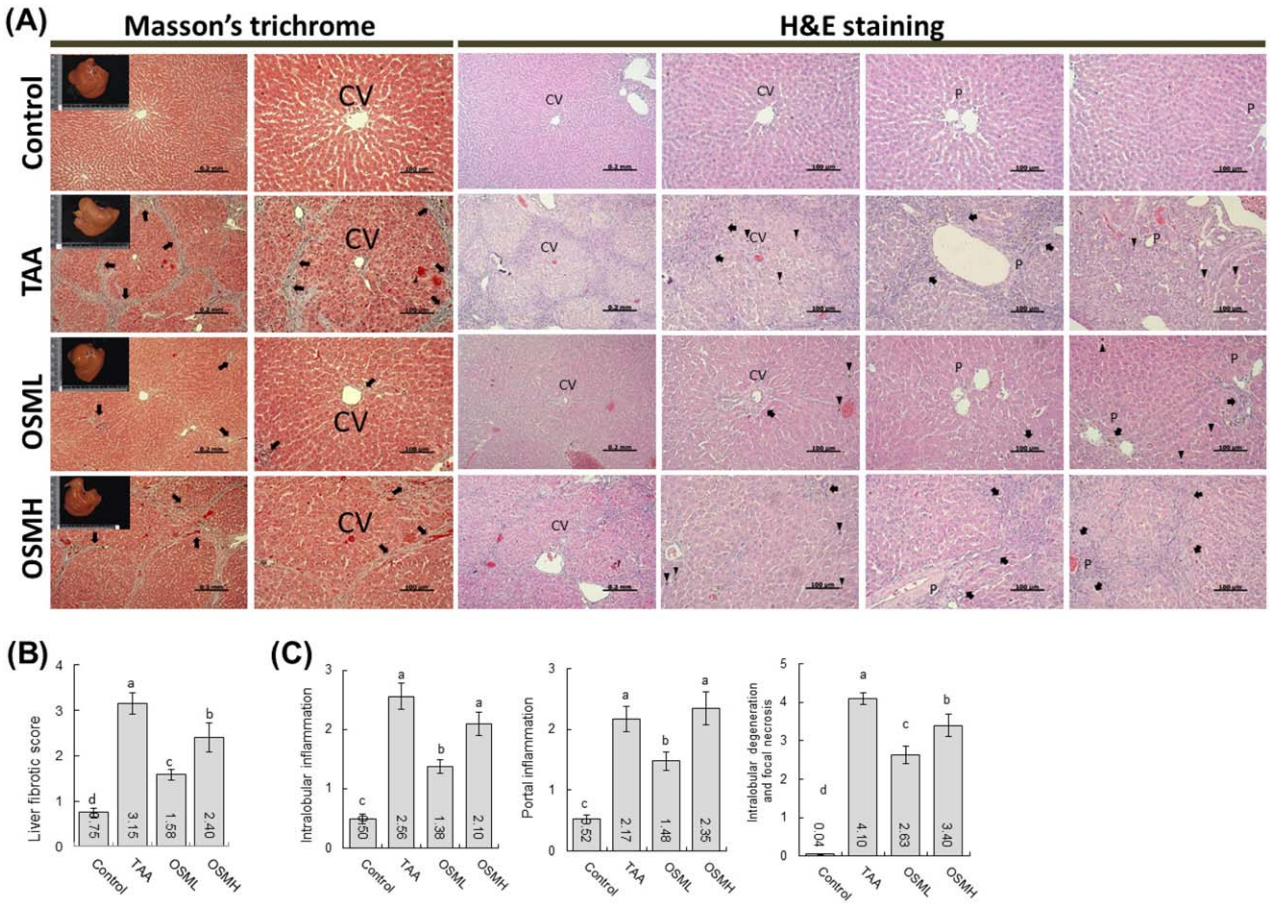

FIGURE 1 Pathohistological analyses for liver tissues. (A) The appearance of representative livers and results of Masson's trichrome and H&E stainings in animals. The scale was shown in 200 (×100) and 100 (×200) μm. CV and *P* were abbreviated names of central vein and portal tracts, respectively, and the triangles in Masson's trichrome were toward to the collagen fibers. In the H&E staining, the black arrows and triangles were toward to inflammation area and necrotic cells, respectively. (B) The score of liver fibrosis. (C) The scores of HAI. * Values of each bar were expressed as mean ± SEM ($n = 12$). ** Data bars without the same letters indicated significant differences ($P < 0.05$) [Color figure can be viewed at wileyonlinelibrary.com]

and intralobular area (Figure 1A). The quantitative results were also similar with the results of Masson's trichrome staining, where the adverse effect, that is, higher fibrotic scores (Figure 1B) as well as liver intralobular and portal inflammation, intralobular degeneration, and focal necrosis (Figure 1C), in TAA-injected rats were reduced ($P < 0.05$) by supplementing OSM.

As aforementioned, TAA-metabolites caused cell damage during development of chronic liver fibrosis.[20] Besides, the covalent binding led to membrane destruction of hepatic cells, and target cells went under necrosis. Consequently, the AST and ALT levels would be released into the extracellular liquid. The oxidative stress and cell death signals trigger many signal transductions such as fibrogenic, immuno and inflammatory response and so forth.[11,24] It has been demonstrated that the mitochondrial damage and lipid peroxidation stimulated Kupffer cells or adjacent sinusoidal endothelial cells to secret cytokines, that is, TNF-α and IL-1β, which lead to sever inflammation[25] and apoptosis.[26] For H&E staining, the visible signs of fibrosis and intrahepatic inflammation were also directly observed (Figure 1A). The scores of inflammation by HAI evaluation also supported that the TAA-intoxication could be ameliorated by OSM supplementation in this study (Table 2 and Figure 1). After all, OSM supplementation would modulate the inflammation via attenuating the pro-inflammatory cytokine secretion.

3.4 | Protective mechanism by OSM supplementation

According to the mRNA expressions of NFκB induction pathways, the TGF-β and TLR4 pathway (Figure 2), TAA treatment significantly upregulated ($P < 0.05$) *Tgfb1*, *Tgfbr1*, and *Tgfbr2*, as well as *Trif* and *Akt*, respectively, while *Tlr4* and *MyD88* gene expressions were not ($P > 0.05$) influenced. Regarding to the fibrosis related gene expressions (Figure 2), *αSMA*, *Col1α*, *NFκB*, and *Cox2* were upregulated ($P < 0.05$) by the TAA intoxication as well. Those changed patterns of gene expressions were downregulated ($P < 0.05$) by OSM supplementation, especially a high dosage of OSM (OSMH group). In the immunohistochemical analyses of αSMA (Figure 3), a general marker of HSC activation, there were more stained αSMA positive cells (triangles and dash circles) in liver tissues of TAA injected groups compared to that of Control group. OSM supplementation significantly reduced them which corresponding to the observations of Masson's trichrome (fibrotic scars in Figure 1). In addition, the less marker protein of hepatic macrophage,

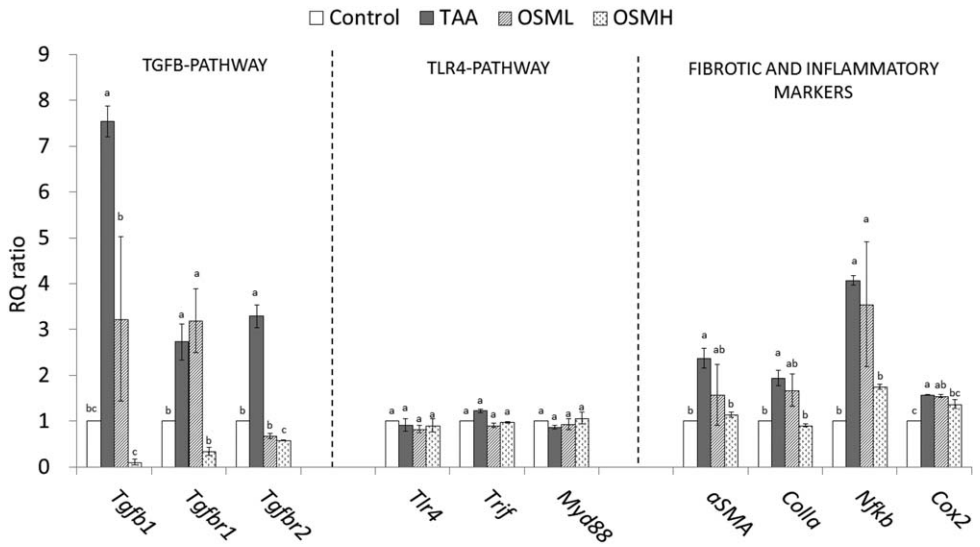

FIGURE 2 mRNA expressions via realtime-PCR for liver tissues. All results were indicated by three clusters as followed: TGF-β related, TLR4 related, and hepatic fibrosis related genes. * The data were given as means ± SEM ($n = 6$, randomly picked up). ** Data bars in each target gene expression without the same letters indicated significant differences ($P < 0.05$)

CD68/ED1 (Figure 3) in OSM-supplemented groups which compared to those in TAA-injected rats without OSM supplementation.

The TGF-β relative pathway is a classic fibrotic signaling cascade in various tissues, and it has been proved to be a necessary factor in the HSC activation.[27] Taylor[28] indicated that pro- and activated-TGF-β molecules are released from ECM via immune cells, such as T-cell, Kupffer cell and so forth. The OSM supplementation could be effective to decrease the inflammation (Table 2 and Figure 1), so it disrupted the downstream signals of TGF-β (Figure 2) and attenuated the HSC activation (Figures 2 and 3). HSCs were activated by ROS and calcium flux which provoked by TGF-β signal cascade;[29] meanwhile, the results in this study clearly indicated that OSM supplementation obviously

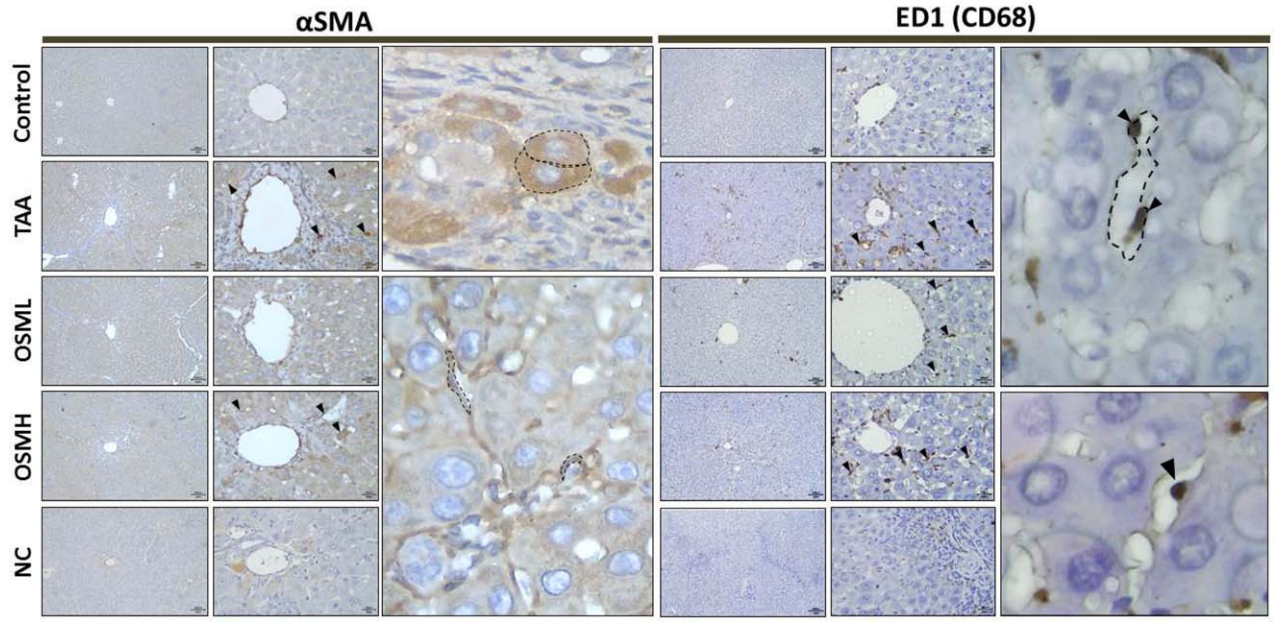

FIGURE 3 2Immunochemical analyses for αSMA and ED1. The results were indicated by each protein: αSMA (left) and CD68/ED1 (right). Respectively, the scales were shown in 20 (×100, first column in left hand) and 100 μm (×400, second column), respectively. Slides were stained with primary antibody and hematoxylin; moreover, the primary antibody was absent in NC (Negative control) group, and the signals were amplified with ABC system. Last, the reaction group of ABC complex turned DAB to brown product. In the stainings of αSMA (left), the expression area (triangles) and cell type (circle in dotted line) were illustrated. The positive areas were in brown color, which may indicate to hepatocytes (upper) and myofibroblast-like cells (lower) depend on its morphology. CD68/ED1 is highly glycosylated lysosomal glycoproteins (LGPs). CD68/ED1 is also found on the surface of macrophages, monocytes, neutrophils, basophils and large lymphocytes. In the right part, it demonstrated the expression area (triangles) and location (hepatic sinusoid in dash-line) [Color figure can be viewed at wileyonlinelibrary.com]

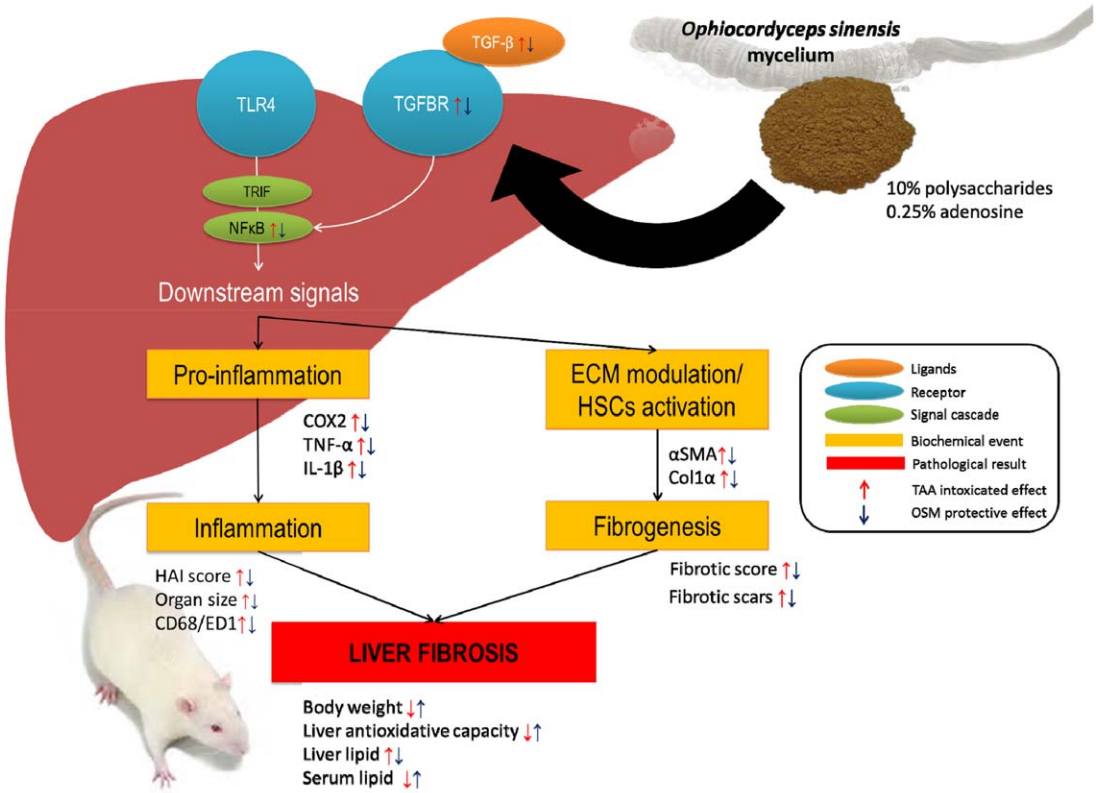

FIGURE 4 Schematic representation of protective mechanism by which *Ophiocordyceps sinensis* mycelium alleviates TAA-induced liver fibrosis [Color figure can be viewed at wileyonlinelibrary.com]

could improve the antioxidative system (Table 1). In addition, NFκB, a key player in controlling both innate and adaptive immunities, was found an apoptotic modulator in livers.[4,30] Although the general function had been revealed, the specific function in the development of liver fibrosis is still lacking due to the various cell types in livers. In the fibroblasts, NFκB is an upstream suppressor of apoptotic signal from extracellular TGF-β.[31] In the activated HSCs, apoptotic signals from TGF-β and TNF-α also involves the downstream of NFκB.[32] Pagliari et al.[33] reported that macrophages require constitutive NFκB activation to maintain survival signals; therefore, the suppression of NFκB signal (Figure 2) should change the dynamics of macrophage (CD68/ED1) (Figure 3) which may attribute to attenuate the macrophage-mediate immune process (Table 2). In our results, the expression pattern of NFκB was altered in OSM supplementation *in vivo* (Figure 2), and the transcription pattern of downstream molecules (i. e., COX2, TNF-α, and IL-1β) are also similar (Table 2 and Figure 2). Consistently, there are fewer stained-positive marker cells of macrophages (CD86/ED1) in livers of TAA-treated rats cotreated with OSM (Figure 3). Hence, the inflammation and immune response may be accompanied by the fibrotic development in the injury process, and the evidence of anti-fibrotic ability (Figures 1–3) supports the aforementioned results in this study. Overall, it can be inferred that OSM decreases the expression of NFκB, thus attenuating the inflammation which downregulates expressions of pro-inflammatory cytokines. Besides, TLR4 signaling participates in chronic liver diseases including hepatic fibrosis.[34] TLR4 signaling is an upstream factor that affects the activation of NFκB. Seki et al.[35] also proved that TLR4 mediates the regulation of TGF-β pseudo-receptor in HSCs. In this study, the receptor and downstream signals (i. e., Trif and MyD88) of TLR4 pathway were not responsive to TAA treatment in mRNA level (Figure 2) which may not participate in the pathway involved in OSM-related preventive effects.

4 | CONCLUSION

According to the current results (Figure 4), the hepatoprotective effects of edible OSM against the TAA treatment are revealed, and the main effect was attributed to reduce liver lipid accumulation and cytokine secretions but increase antioxidative capabilities. Protective effects of OSM against the TAA intoxication also involve the NFκB signal and TGF-β related pathway. Comprehensively, not only observations of physiological values but also investigation of antioxidative and anti-inflammatory/anti-fibrotic mechanisms on OSM supplementation against TAA-induced liver fibrosis were mentioned in this study. However, it seems to be dose-independent. Although results of OSMH may not effective as those of OSML, its hepatoprotective effect is still presented compared to TAA group. Therefore, it showed that OSM is capable of modulating TGF-β and NFκB signals via direct or indirect effects. The results should apparently demonstrate solid evidence on health benefits of OSM on livers to the consumers.

REFERENCES

[1] Weber LW, Boll M, Stampfl A. Hepatotoxicity and mechanism of action of haloalkanes: carbon tetrachloride as a toxicological model. *Crit Rev Toxicol*. 2003;33:105–136.

[2] Childs JFL, Siegler EA. Uses of thioacetamide in agriculture. *Science*. 1945;102:68–72.

[3] Chieli E, Malvaldi G. Role of the microsomal FDA-containing monooxygenase in the liver toxicity of thioacetamide S-oxide. *Toxicology*. 1984;31:41–52.

[4] Chen PX, Wang S, Nie S, Marcone M. Properties of *Cordyceps sinensis*: a review. *J Funct Foods*. 2013;5:550–569.

[5] Cheng YJ, Cheng SM, Teng YH, Shyu WC, Chen HL, Lee SD. *Cordyceps sinensis* prevents apoptosis in mouse liver with d-galactosamine/lipopolysaccharide-induced fulminant hepatic failure. *Am J Chin Med*. 2014;42:427–441.

[6] Liu YK, Shen W. Inhibitive effect of *Cordyceps sinensis* on experimental hepatic fibrosis and its possible mechanism. *World J Gastroenterol*. 2003;9:529–533.

[7] Meng LZ, Feng K, Wang LY, et al. Activation of mouse macrophages and dendritic cells induced by polysaccharides from a novel *Cordyceps sinensis* fungus UM01. *J Funct Foods*. 2014;9:242–253.

[8] Peng Y, Chen Q, Yang T, Tao YY, Lu X, Liu CH. Cultured mycelium *Cordyceps sinensis* protects livers sinusoidal endothelial cells in acute liver injured mice. *Mol Biol Rep*. 2014;41:1815–1827.

[9] Peng JH, Li XM, Feng Q, Chen LL, Xu L, Hu YY. Anti-fibrotic effect of *Cordyceps sinensis* polysaccharide: inhibiting HSC activation, TGF-β1/Smad signaling, MMPs and TIMPs. *Exp Biol Med*. 2013;238:668–677.

[10] Yue K, Ye M, Zhou Z, Sun W, Lin X. The genus *Cordyceps*: a chemical and pharmacological review. *J Pharm Pharmacol*. 2012;65:474–493.

[11] Fang YJ, Chiu CH, Chang YY, et al. Taurine ameliorates alcoholic steatohepatitis via enhancing self-antioxidant capacity and alcohol metabolism. *Food Res Int*. 2011;44:3105–3110.

[12] Brunt EM. Grading and staging the histopathological lesions of chronic hepatitis: the knodell histology activity index and beyond. *Hepatology*. 2000;31:241–246.

[13] Ljubuncic P, Song H, Cogan U, Azaizeh H, Bomzon A. The effects of aqueous extracts prepared from the leaves of *Pistacia lentiscus* in experimental liver disease. *J Ethnopharmacol*. 2005;100:198–204.

[14] Snyder CK, Lapidus JA, Cawthon PM, Dam TL, Sakai LY, Marshall LM. Serum albumin in relation to change in muscle mass, muscle strength, and muscle power in older men. *J Am Geriatr Soc*. 2012;60:1663–1672.

[15] Water NJ, Waterfield CJ, Farrant RD, Holmes E, Nicholson JK. Metabonomic deconvolution of embedded toxicity: application to thioacetamide hepato- and nephrotoxicity. *Chem Res Toxicol*. 2015;18:639–654.

[16] Natarajan SK, Basivireddy J, Ramachandran A, et al. Renal damage in experimentally induced cirrhosis in rats: role of oxygen free radicals. *Hepatology*. 2006;43:1248–1256.

[17] Hocher B, Heiden S, von Websky K, et al. Renal effects of the novel selective adenosine A1 receptor blocker SLV329 in experimental liver cirrhosis in rats. *PLoS One*. 2011;6:e17891.

[18] Kang JS, Wanibuchi H, Morimura K, et al. Role of CYP2E1 in thioacetamide-induced mouse hepatotoxicity. *Toxicol Appl Pharmacol*. 2008;228:295–300.

[19] Chen IS, Chen YC, Chou CH, Chuang RF, Sheen LY, Chiu CH. Hepatoprotection of silymarin against thioacetamide-induced chronic liver fibrosis. *J Sci Food Agric*. 2011;92:1441–1447.

[20] Kaplowitz N. Drug-induced liver injury. *Clin Infect Dis*. 2004;38:S44–S48.

[21] Chen PJ, Chiu CH, Tseng JK, Yang KT, Chen YC. Ameliorative effects of d-glucuronolactone on oxidative stress and inflammatory/fibrogenic responses in livers of thioacetamide-treated rats. *J Funct Foods*. 2015;14:154–162.

[22] Ko WS, Hsu SL, Chyau CC, Chen KC, Peng RY. Compound Cordyceps TCM-700C exhibits potent hepatoprotective capability in animal model. *Fitoterapia*. 2010;81:1–7.

[23] Kumar R, Negi PS, Singh B, Ilavazhagan G, Bhargava K, Sethy NK. *Cordyceps sinensis* promotes exercise endurance capacity of rats by activating skeletal muscle metabolic regulators. *J Ethnopharmacol*. 2011;136:260–266.

[24] Jaeschke H, Gores GJ, Cederbaum AI, Hinson JA, Pessayre D, Lemasters JJ. Mechanisms of hepatotoxicity. *Toxicol Sci*. 2002;65:166–176.

[25] Shakibaei M, Schulze-Tanzil G, Takada Y, Aggarwal BB. Redox regulation of apoptosis by members of the TNF superfamily. *Antioxid Redox Signal*. 2005;7:482–496.

[26] Meier P, Silke J. Programmed cell death: superman meets Dr Death. *Nat Cell Biol*. 2003;5:1035–1038.

[27] Dewidar B, Soukupova J, Fabregat I, Dooley S. TGF-β in hepatic stellate cell activation and liver fibrogenesis: updated. *Curr Pathobiol Rep*. 2015;3:291–305.

[28] Taylor AW. Review of the activation of TGF-β in immunity. *J Leukoc Biol*. 2009;85:29–33.

[29] Yang KL, Chang WT, Chuang CC, Hung KC, Li EIC. Antagonizing TGF-β induced liver fibrosis by a retinoic acid derivative through regulation of ROS and calcium influx. *Biochem Biophys Res Commun*. 2008;365:484–489.

[30] Chang YY, Lin YL, Yang DJ, et al. Hepatoprotection of noni juice against chronic alcohol consumption: lipid homeostasis, antioxidation, alcohol clearance, and anti-inflammation. *J Agri Food Chem*. 2013;61:11016–11024.

[31] Bitzer M, Gersdorff GV, Liang D, et al. A mechanism of suppression of TGF-β/SMAD signaling by NFκB/RelA. *Genes Dev*. 2000;14:187–197.

[32] Saile B, Matthes N, Armouche HE, Neubauer K, Ramadori G. The bcl, NFκB and p53/p21^{WAF1} systems are involved in spontaneous apoptosis and in the anti-apoptotic effect of TGF-β or TNF-α on activated hepatic stellate cells. *Eur J Cell Biol*. 2001;80:554–561.

[33] Pagliari LJ, Perlman H, Liu H, Pope RM. Macrophages require constitutive NF-κB activation to maintain A1 expression and mitochondrial homeostasis. *Mol Cell Biol*. 2000;20:8855–8865.

[34] Guo J, Friedman SL. Toll-like receptor 4 signaling in liver injury and hepatic fibrogenesis. *Fibrogenesis Tissue Repair*. 2010;3:21–36.

[35] Seki E, De Minicis S, Osterreicher CH, et al. TLR4 enhances TGF-beta signaling and hepatic fibrosis. *Nat Med*. 2007;13:1324–1332.

How to cite this article: Wu Y-HS, Tseng J-K, Chou C-H, Chiu C-H, Lin Y-L, Chen Y-C. Preventive effects of *Ophiocordyceps sinensis* mycelium on the liver fibrosis induced by thioacetamide. *Environmental Toxicology*. 2017;32:1792–11800. https://doi.org/10.1002/tox.22402